(1969) *J. Mol. Biol. 39*, 279–292.
Record, M. T., Jr., Lohman, T. M., & de Haseth, P. L. (1976) *J. Mol. Biol. 107*, 145–158.
Record, M. T., Jr., de Haseth, P. L., & Lohman, T. M. (1977) *Biochemistry 16*, 4791–4795.
Riggs, A. D., Bourgeois, S., & Cohn, M. (1970) *J. Mol. Biol. 53*, 401–417.
Strauss, H. S., Burgess, R. R., & Record, M. T., Jr. (1980) *Biochemistry 19*, 3504–3515.
von Hippel, P. H. (1979) in *Biological Regulation and Development* (Goldberger, R. F., Ed.) pp 279–347, Plenum Press, New York.
von Hippel, P. H., & Schleich, T. (1969) in *Structure and Stability of Biological Macromolecules* (Timasheff, S., & Fasman, G., Eds.) pp 417–574, Marcel Dekker, New York.
Weber, K. (1967) *Biochemistry 6*, 3144–3154.
Winter, R. B., Berg, O. G., & von Hippel, P. H. (1981) *Biochemistry 20*, 6960–6970.

Nuclear Overhauser Experiments at 500 MHz on the Downfield Proton Spectrum of a Ribonuclease-Resistant Fragment of 5S Ribonucleic Acid†

M. J. Kime and P. B. Moore*

ABSTRACT: The downfield (9–15 ppm) proton NMR spectrum of a RNase A resistant fragment of *E. coli* 5S RNA has been studied by nuclear Overhauser methods. The fragment comprises bases 1–11 and 69–120 of the parent molecule [Douthwaite, S., Garrett, R. A., Wagner, R., & Feunteun, J. (1979) *Nucleic Acids Res. 6*, 2453–2470]. The nuclear Overhauser data identify two double helical structures in the fragment whose sequences are $(GC)_3(AU)(GC)_3$ and $(GC)_2(AU)(GU)$. These structures correspond exactly to the central portions of the terminal stem and procaryotic loop helices which should exist in the fragment sequences according to the Fox–Woese model [Fox, G. E., & Woese, C. R. (1975) *Nature (London) 256*, 505–506] of 5S RNA secondary structure. The significance of these and other nuclear Overhauser effects detected for the structure of 5S RNA and its fragment is discussed.

5S ribonucleic acid and its complexes with ribosomal protein constitute a convenient, low molecular weight system in which the general problem of the interactions of proteins with RNA may be examined. Since the discovery of this molecule in the early 1960s (Rosset & Monier, 1963) a wide variety of genetic, chemical, and physical experiments have been done in an effort to elucidate its structure and the nature of its interactions with proteins [for review see Monier (1974), Zimmermann (1980), and Garrett et al. (1981)]. Among the physical methods brought to bear on this problem has been nuclear magnetic resonance (NMR).

Around 1970 it was demonstrated that nucleic acids dissolved in H_2O give proton resonances between 10 and 15 ppm due to hydrogen-bonded imino protons in base pairs (Kearns et al., 1971a,b). Since relative to the total number of protons in a nucleic acid molecule so few protons contribute resonances in this region, and since the protons which resonate in this region are directly involved in the interactions which stabilize nucleic acid structure, it was clear that interpretation of the downfield region of a nucleic acid proton NMR spectrum was likely to be both feasible and revealing. Work on this kind of spectroscopy has been vigorously pursued ever since [for reviews see Kearns & Shulman (1974), Kearns (1976, 1977), Reid & Hurd (1977), Schimmel & Redfield (1980), and Reid (1981)].

While tRNAs have been the natural nucleic acids which have received the most attention from NMR spectroscopists, 5S RNA, the next largest, abundant RNA, has also been examined. The goal of most proton NMR studies on 5S RNA has been to determine the number of hydrogen bonds in that molecule under different conditions (Wong et al., 1972; Kearns & Wong, 1974; Burns et al., 1980; Luoma et al., 1980; Salemink et al., 1981). In many cases ring current shift calculations have been done to test models of 5S structure against observed downfield proton spectra. Specific resonances in the downfield spectrum of 5S, however, have not been assigned. The downfield spectra given by 5S RNA samples are substantially less well resolved than those of most tRNAs. Given the difficulties which have beset the assigning of tRNA imino resonances until very recently [see Reid (1981), Roy & Redfield (1981), Sanchez et al. (1980), and Schimmel & Redfield (1980)], it hardly seemed worthwhile to pursue assignments in 5S RNA. Without detailed assignments, of course, much of the information which could be gained from studies of the 5S downfield spectrum is lost.

Three years ago it was shown that a large fragment of 5S RNA from *E. coli* can be obtained from it by limited nuclease digestion. The fragment is about half the molecule, consisting of bases 1–11 and 69–120 (Douthwaite et al., 1979), usually with some breakage at bases 87, 88, or 89. Recently it was shown that this fragment has a structure remarkably similar to that of the same sequences in the intact molecule (Kime & Moore, 1983). Its downfield NMR spectrum is a subset of the spectrum of the whole molecule; all structures giving rise to observable downfield features in the fragment spectrum must also exist in the parent molecule. Because the fragment spectrum has fewer resonances and its line widths are narrower, it is far easier to work with than that of the parent molecule. The study of the 5S fragment spectrum offers a means for understanding the structure of the parent molecule, just as the study of nucleolytic fragments of tRNA assisted in the understanding of tRNA spectra (Lightfoot et al., 1973; Kearns & Shulman, 1974; Reid et al., 1979).

† From the Department of Chemistry, Yale University, New Haven, Connecticut 06511. *Received December 13, 1982.* This research was supported by a grant from the National Institutes of Health (AI-09167) to P.B.M. M.J.K. is a NATO/SERC postdoctoral fellow.

0006-2960/83/0422-2615$01.50/0

In the last few years those studying tRNAs by NMR have shown that nuclear Overhauser effect (NOE) techniques constitute a powerful tool for interpreting nucleic acid downfield spectra (Johnston & Redfield, 1978, 1981; Sanchez et al., 1980; Roy & Redfield, 1978, 1981; Sanchez et al., 1980; Roy & Redfield, 1981; Hare & Reid, 1982a,b). Below we report the results of series of NOE experiments done on the RNAse-resistant fragment of 5S RNA from *Escherichia coli*. The data establish tentative assignments for a large number of resonances in the fragment spectrum and suggest the existence of two helical segments in the molecule which correspond in sequence to the terminal stem and the procaryotic loop helices proposed for intact 5S RNA by Fox & Woese (1975) and others. Given the similarity of the fragment spectra and those of its parent molecule, these results are the first physical evidence for the existence of these structures in 5S RNA.

Materials and Methods

Ribosomal 5S RNA. 5S RNA was prepared from 70S ribosomes or 50S subunits (*E. coli* MRE 600) as described elsewhere (Kime & Moore, 1982). 5S RNA from *E. coli* B was obtained from total, cellular, low molecular weight RNA purchased from Plenum Scientific Research, Hackensack, NJ. 5S RNA was purified from this mixture by chromatography on Sephacryl S-200 at room temperature in 0.15 M NaCl, 1% methanol, and 0.1 M sodium acetate, pH 5.0. One gram of RNA was applied in a 20-mL sample to a 5 cm × 100 cm column. The yield was 5–7% by weight of the starting material.

rrnB 5S RNA. HB101/pKK5-1 is an *E. coli* strain which carries the rrnB 5S RNA cistron on a plasmid (pBR322) (Brosius et al., 1981). In order to obtain large quantities of rrnB 5S RNA, the strain was grown on L broth supplemented with 50 μg/mL ampicillin, 15 μg/mL thiamin, 0.5 mg/mL adenosine, and 0.5 mg/mL uridine at 37 °C. When the apparent optical density of the culture reached 2.0 at 550 nm, 50 μg/mL chloramphenicol was added and the growth continued for 4–5 h more. Following harvest the cell paste was ground with alumina and a postribosomal supernatant prepared by centrifugation at 45 000 rpm for 3 h at 4 °C in a Ti 45 rotor. The supernatant was phenol extracted and the RNA recovered by ethanol precipitation. 5S material was purified by chromatography on Sephacryl S-200 as described above. The yield is up to 15 mg of 5S RNA/L of culture.

Fragment Preparation. 5S RNA was dissolved in 0.1 M KCl, 5 mM $MgCl_2$, and 50 mM Tris–borate,[1] pH 7.8, at 20 OD_{260nm}/mL. RNase A (Worthington) was added at a concentration of 10 μg/mL. After 45 min at 0 °C the reaction was terminated by the addition of sodium dodecyl sulfate followed immediately by phenol extraction. The fragment was purified by chromatography on Sephadex G-75 in 0.1 M NaCl, 3 mM $MgCl_2$, and 10 mM cacodylate, pH 6.0 at 30 °C.

The purity of this material was checked by acrylamide gel electrophoresis on gels consisting of 10% acrylamide, 0.5% bis(acrylamide), 0.08% TEMED, and 0.50% ammonium persulfate. The buffer was 0.1 M KCl, 5 mM $MgCl_2$, and 50 mM Tris–borate, pH 7.8. Gels were run at 3V/cm for 16 h at room temperature, and RNA was visualized by staining with methylene blue.

L25. The preparation of ribosomal protein L25 has been described elsewhere (Kime et al., 1981; Kime & Moore, 1982).

NMR Samples. Fragment preparations were dialyzed against 0.1 M KCl, 4 mM $MgCl_2$, and 5 mM cacodylic acid, pH 7.18 in 5% D_2O. They were then concentrated to a volume of 0.5 mL by ultrafiltration using a YM5 membrane (Amicon). Two microliters of 1 M dioxane in H_2O was added to each sample as a chemical shift reference. The proton resonance of dioxane is assumed to have a chemical shift of 3.741 ppm relative to the methyl resonance of 3-(trimethylsilyl)-1-propanesulfonic acid.

NMR Spectroscopy. All spectra were accumulated on a Bruker WM 500 NMR spectrometer operating in the Fourier transform mode. Spectra were measured at 303 K unless stated otherwise. Lower temperatures were maintained with a flow of dry N_2 gas precooled by passage through heat-exchange coils immersed in a propan-2-ol dry ice mixture. Water proton contributions to the spectrum were suppressed by use of a (45°–*t*–45°) observation pulse sequence. The total time for the pulse train was 110 μs and the F1 frequency was offset about 5560 Hz downfield of water. All difference spectra and absolute intensity spectra were accumulated by using a pulse cycle time of 5 s and 32K memory blocks for data storage. For NOE data collection a presaturation pulse length of 200 ms and 8K of memory were used, giving a total pulse cycle time of 0.4 s. NOE spectra were accumulated in an interleaved fashion with an operating cycle of 16 passes with F2 on-resonance followed by 16 passes with F2 off-resonance. Differences were computed after storage of on- and off-resonance free induction decays.

Results

Fragment Samples. In the course of this work, RNase-resistant 5S RNA fragment was made from 5S RNA prepared in a variety of ways. Initially 70S ribosomes or 50S subunits from *E. coli* MRE 600 were used as the 5S source. Some use was also made of 5S RNA purified from commercial, low molecular weight RNA obtained by phenol extraction of whole cells (*E. coli* B). The fragment preparations made from these different ribosomal 5S RNA were electrophoretically and spectroscopically indistinguishable and will be called "ribosomal 5S RNA".

In the later stages of the work *E. coli* HB101/pKK5-1 was used as a 5S RNA source. This strain, kindly given to us by Drs. J. Brosius and H. F. Noller, carries the rrnB 5S RNA cistron on a plasmid, and it can overproduce 5S RNA about 20-fold. The purification of 5S RNA from this material involved fractionation of the postribosomal RNAs by chromatography on Sephacryl S-200. Figure 1 shows an electrophoretic comparison of postribosomal RNA from HB101/pKK5-1 at an early stage in overproduction (lane a), with pure ribosomal 5S RNA in the A form (lane b), and with purified rrnB 5S (lane c). It is clear that the rrnB 5S product migrates slightly slower than ribosomal 5S RNA. In fact its sequence is not normal; it is about five bases longer than ribosomal 5S RNA at the 5′ end (H. Noller, personal communication). 50S subunit reconstitutions have been done to test the functional properties of rrnB 5S RNA; it does substitute for the mature ribosomal 5S RNA in reconstitutions (P. B. Moore, unpublished results).

Lanes d–g of Figure 1 show the outcome of an electrophoretic experiment on the production of fragment from rrnB 5S RNA. Lane d is a sample of unpurified rrnB digest which is compared to ribosomal 5S fragment (lane e). In the presence of an excess of L25 the main component in the digest shows a reduced mobility (lane g) which is identical with that of ribosomal fragment under the same circumstances (lane f). Reduced mobility indicates binding to L25 (Douthwaite et al.,

[1] Abbreviations: Tris, tris(hydroxymethyl)aminomethane; TEMED, *N,N,N′,N′*-tetramethylethylenediamine.

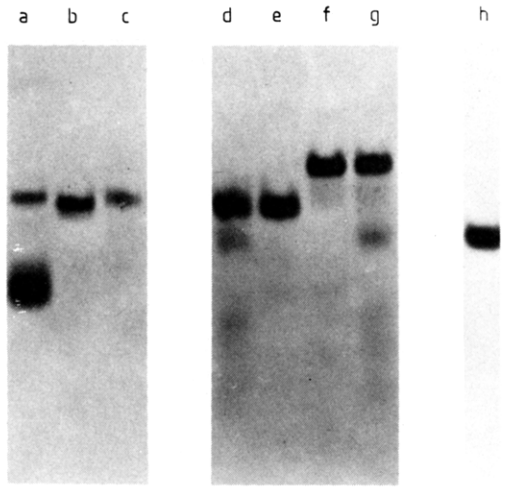

FIGURE 1: Acrylamide gel results with rrnB 5S RNA and 5S RNA fragment. Three experiments are shown all run under similar gel conditions [10% acrylamide, 0.5% bis(acrylamide), 0.08% TEMED, 0.05% ammonium persulfate, 0.1 M KCl, 5 mM $MgCl_2$, and 50 mM Tris–borate, pH 7.8]. Runs were done at 3 V/cm overnight, and the buffer was recirculated to stabilize the pH. Experiment 1: The low molecular weight RNA of HB101/pKK5-1 at an early stage of overproduction (lane a) is compared with pure ribosomal 5S RNA (lane b) and rrnB 5S RNA (lane c). The loading was about 0.3 A_{260nm} for lane a and 0.15 A_{260nm} for lanes b and c. Electrophoresis was done at 23 °C. Experiment 2: 0.3 A_{260nm} of rrnB 5S RNA was digested for 45 min at 0 °C with 0.15 μg of RNase A in the gel buffer described above and the total digest applied to the gel (lane d). Lane e shows the result of electrophoresis of 0.15 A_{260nm} of purified ribosomal 5S RNA fragment. Lanes f and g are repeats of lanes d and c with 6 μg of L25 added to each. Electrophoresis was carried out at 4 °C. Experiment 3: 0.15 A_{260nm} of purified rrnB 5S RNA fragment was run at room temperature for 16 h at 3 V/cm (lane h).

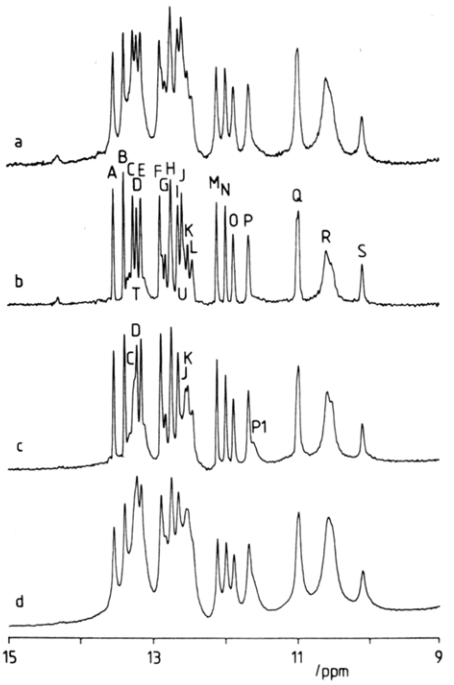

FIGURE 2: Downfield proton spectra of ribosomal and rrnB fragment RNA. Spectrum a: A 1 mM sample of ribosomal fragment at pH 7.2, 30 °C in the presence of 4 mM $MgCl_2$ and 0.1 M KCl. Spectrum accumulated with a 5-s cycle time. Spectrum b: A resolution-enhanced version of spectrum a with resonances designated with letters. Spectrum c: Spectrum d, resolution enhanced. Those resonances whose chemical shifts differ from their correspondents in spectrum b are noted. Spectrum d: A 2.5 mM sample of rrnB fragment. The conditions are identical with those used in accumulating spectrum a.

1979; Kime & Moore, 1982). The two types of fragment are indistinguishable by electrophoretic criteria. Lane h of Figure 1 shows that that fragment can be purified satisfactorily by chromatography on Sephadex G-75.

Spectroscopic Comparison of rrnB and Ribosomal Fragment. Downfield spectra were accumulated on samples of the rrnB fragment and of the ribosomal fragment under identical conditions. Figure 2a is the ribosomal fragment spectrum and Figure 2b is the same spectrum, resolution enhanced. Parts d and c of Figure 2 are the corresponding spectra for the rrnB fragment. Resonances are identified by letter for further reference.

The two preparations give spectra which are similar, but not identical. In the rrnB fragment peaks C and J have chemical shifts which place them slightly upfield of the corresponding resonances in the ribosomal fragment. All the resonances in both forms of fragment have been studied by NOE methods (see below). The data show that resonances designated with the same letter in the two spectra come from corresponding protons in the two structures and that the two structures are similar.

The spectral differences between the two kinds of fragments must reflect sequence differences. These could either be a consequence of the fact that rrnB 5S RNA is not fully mature when it is made into fragment or be due to the fact that the 5S RNA from normal cells is a sampling of the products from seven 5S RNA cistrons differing slightly in sequence (Brownlee et al., 1968; Jarry & Rosset, 1971) while the rrnB product approaches a pure preparation of just one such species. Experiments are under way to resolve this point.

NOE Strategy. As the tRNA spectroscopists have elegantly demonstrated, when hydrogen-bonded imino proton resonances are presaturated, measureable NOEs are generally seen only to nearest-neighbor protons in a double helix. In the case of standard Watson–Crick GC base pairs, among the nearest neighbors are the hydrogen-bonded imino protons of the base pairs immediately above and below the base pair whose imino proton is being saturated, if they exist (Johnston & Redfield, 1981). There is transfer to nearby amino protons also, but these give weak, broad resonances in the aromatic region around 8 ppm. The imino NOEs of a GC base pair, therefore, identify resonances of the imino protons of its neighboring base pairs.

Presaturation of the imino proton in either a standard Watson–Crick type or reversed Hoogsteen type AU base pair likewise will produce NOEs to the imino protons of its nearest-neighbor base pairs. In addition there is a strong (20%) NOE to a proton on the A of the same pair (Sanchez et al., 1980) which is either the C2 proton for a Watson–Crick pair or the C8 proton for a Hoogsteen pair. This proton gives a sharp, strong resonance in the aromatic region, allowing one to distinguish resonances in the imino region which come from AU base pairs from those arising from CGs, which lack such an upfield correlate. GU wobble base pairs also have a distinctive NOE signature (Johnson & Redfield, 1978; Roy & Redfield, 1981). GUs have two hydrogen-bonded imino protons which generally resonate on the upfield side of the imino region around 11 ppm. A GU base pair imino resonance will give a strong NOE to the other intra base pair imino resonance as well as weaker, but still relatively strong, NOEs to the imino protons of its neighboring base pairs.

Thus NOE experiments allow one to progress through a double-helical region in a nucleic acid identifying the resonance which comes from neighboring base pairs and distinguishing their chemical nature (Hare & Reid, 1982a,b). This information combined with the sequence of the molecule under

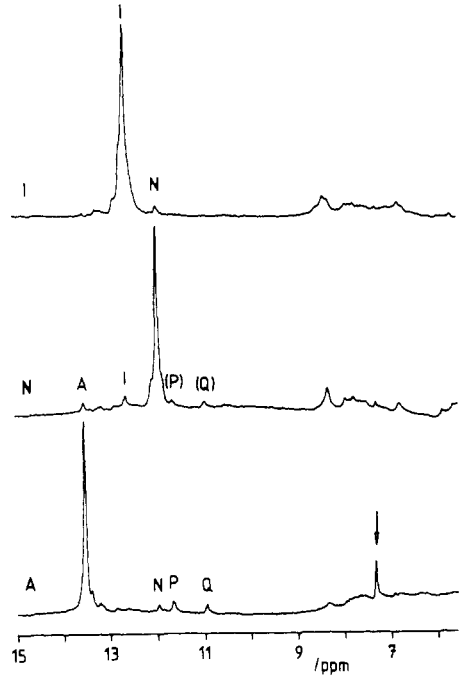

FIGURE 3: NOEs of resonances related to resonance A. A 2.5 mM sample of rrnB fragment was examined for downfield NOEs at 30 °C, pH 7.2 (see Materials and Methods). Each spectrum is labeled with the name of the resonance presaturated. The spectra shown are NOE difference spectra. The resonances elicited by NOE in each spectrum are labeled; the biggest feature in each one is the presaturated resonance. The arrow at about 7.2 ppm cells attention to a sharp, intense NOE in the aromatic region.

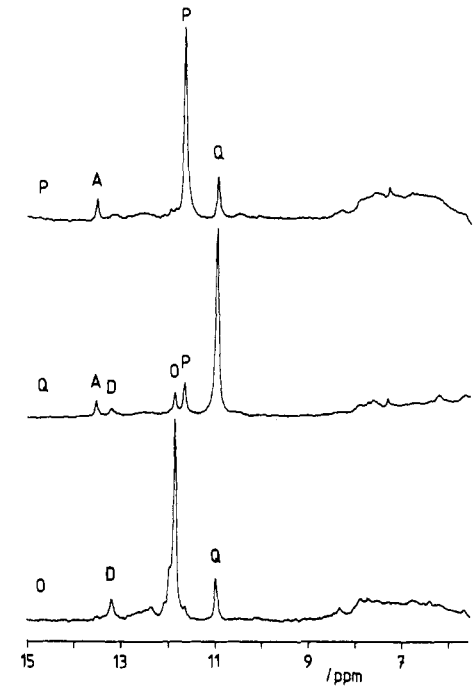

FIGURE 4: Further NOEs of resonances related to resonance A (see legend for Figure 3).

study often allows one to infer which bases are responsible for the secondary structures detected. It is this approach which will be followed below.

NOEs/Resonances Related to Resonance A. A sample of rrnB fragment was prepared at a concentration of 2.5 mM at pH 7.2 in 4 mM $MgCl_2$ at 30 °C. All peaks visible in the spectrum shown in Figure 2 were presaturated and transfer of saturation from the affected proton to its nearest-neighboring protons detected by the now standard NOE difference technique.

Figures 3 and 4 show a typical progression in the rrnB imino spectrum. Each of the spectra is an NOE difference spectrum designated by the letter of the peak which was presaturated in the experiment, which is the strongest feature in each difference spectrum. It is convenient to start with resonance I. Resonance I is probably a GC base pair at the end of a double-helical segment because no strong upfield feature is seen upon presaturation, and only one imino NOE. When N, the resonance connected by NOE to I, is irradiated, I is elicited as expected and a new resonance, A, appears. NOEs are also seen in the N spectrum to resonances P and Q. Since P and Q also appear in the next NOE experiment, the one involving resonance A, it appears that saturation is being transferred efficently from N through A on to P and Q. Because presaturation of N produces no sharp, strong feature in the aromatic region, N is also likely to be a GC. Presaturation of A, on the other hand, does elicit an upfield feature of this kind; A must be an AU base pair imino proton resonance. When P is presaturated, an NOE to Q is seen of unusual strength, suggesting intrabase transfer of saturation. Resonance P also relates to A as expected. Presaturation of Q brings up P strongly, but also A, consistent with the view that P and Q are the two imino protons of a GU base pair which is adjacent to the AU base pair of A, and which ends a helical stack. This assignment is consistent with the chemical shifts of P and Q.

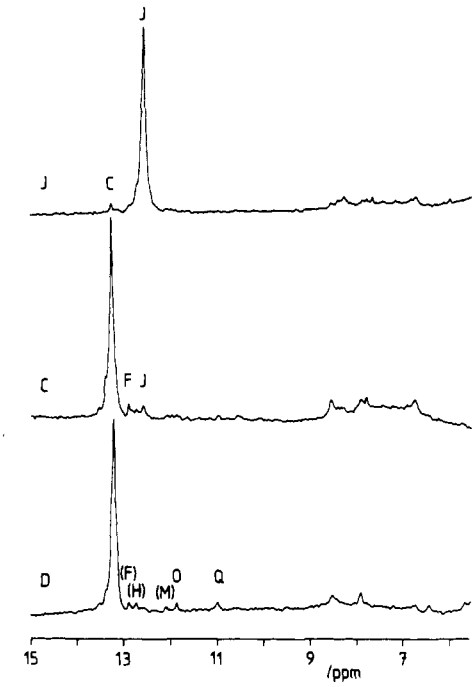

FIGURE 5: Selected NOEs of ribosomal fragment. A number of NOEs are shown which were obtained on a 1.1 mM sample of ribosomal fragment. The conditions for data collection and the presentation of results are as given for Figure 3.

There are two other NOEs from Q, (C, D) and O. In order to decide whether it is C or D which relates to Q, NOE experiments were done on a 1.1 mM sample of ribosomal fragment in which C and D are distinguishable by chemical shift. The key spectra are shown in Figure 5. It is D that relates to O and Q, not C. [The "extra" resonances seen in the D spectrum in Figure 5 are due to overlap of D with C and E which flank it on either side (see Figure 2).] Furthermore, presaturation of O brings up Q strongly as well as D (Figure 4). Thus resonances I, N, A, P, and Q define a helical region which appears to go $(GC)_2(AU)(GU)$ while D,

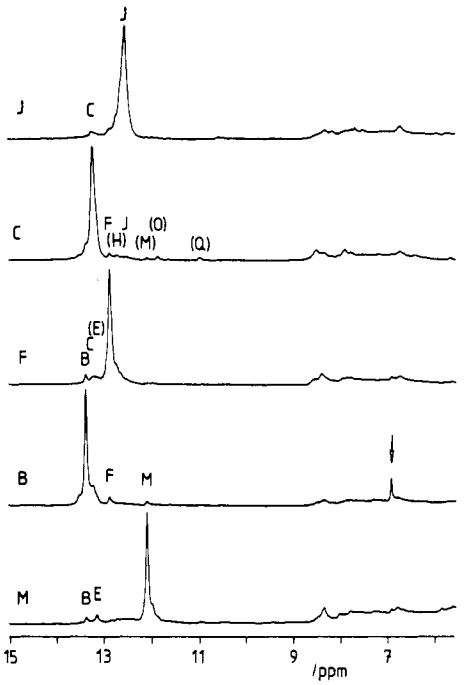

FIGURE 6: NOEs in the rrnB fragment related to resonance B (see legend for Figure 3).

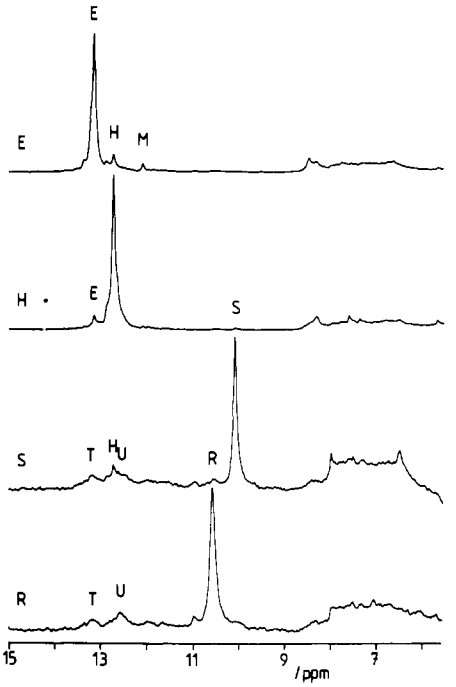

FIGURE 7: Further NOEs related to resonance B (see legend for Figure 3).

O, and Q represent a short segment (GU)(GC) which is unconnected to anything else in the sequence by NOE under these conditions. (The helical sequence is written with each base pair in parentheses to indicate that the NMR data do not permit one to decide which base within a pair goes with which strand of the double helix.) Resonance Q is a chance superposition of two resonances.

NOEs/Resonances Related to Resonance B. There is a second progression possible in the fragment spectrum illustrated by the data in Figures 6 and 7. It is best started at resonance J (Figure 6). Presaturation of J brings up a single NOE to (C, D), suggesting that J is a base pair which ends a helix. Experiments done on ribosomal fragment (Figure 5) show that the resonance affected by J is C, not D. The reverse NOE, C to J, is relatively easy to show in the ribosomal fragment (Figure 5) but harder to demonstrate in the rrnB fragment (Figure 6) where the effect is weaker and tends to be obscured due to nonselectivity in the presaturation pulse which brings up resonances related to D and E as well. Resonance C appears to be a GC base pair situated between the base pairs represented by F and J. It is interesting to note that C and J are the two resonances whose chemical shifts are the most affected by the sequence differences between the rrnB and ribosomal fragment.

Presaturation of F elicits C and a new resonance, B. Again F is a GC by virtue of the absence of a sharp, strong upfield NOE. When B is presaturated, on the other hand, an upfield signal is seen identifying B as an AU base pair. In addition it is clear that B's neighbors are F and M. Continuation of the series yields the sequence M, E, and H, all GC base pairs, giving a helical region of the form $(GC)_3(AU)(GC)_3$ starting with resonance J and ending with H.

Other NOEs. It should be noted that in all fragment samples studied a weak NOE relating a resonance at location E with a resonance at position F is detected. The transfer "F" to "E" is easy to demonstrate; the reverse, "E" to "F", is harder because of the proximity of C to E, C being a resonance which transfers efficiently to F. We are unable to assign this feature at this stage in the analysis.

There are a number of other NOEs seen in the fragment spectrum which cannot be assigned at this point. When R is presaturated, NOEs are elicited from the two broad resonances T and U. When the data obtained by irradiating I, J, K, and L, which lie on top of U, are examined, a weak effect to R is noted which is probably the reverse NOE, U to R. A similar examination of the C, D, and E NOEs does not reveal an NOE to R; the T to R effect anticipated is not seen.

Presaturation of S again reveals T and U, but included in the U feature there is a definite peak at H. There is no evidence for T or U back to S. There is, however, a very weak H to S NOE seen consistently. In intact 5S RNA, the S to H effect is conspicuous, but the reverse H to S is not observable (unpublished observations).

Finally it should be noted that there are three resonances, G, K, and L, for which no NOEs have yet been detected.

NOEs at Low Temperature. All the data described thus far were taken at 30 °C. It seemed possible that at this temperature exchange of imino protons with solvent protons in some base pairs might be fast enough to limit the efficiency of the NOEs we were trying to observe. Accordingly in an effort to extend our assignments, a series of experiments were performed at 10 °C, where exchange effects are expected to be reduced.

Figure 8 compares the spectrum of rrnB fragment at 10 °C (spectra d and c) with that of the same molecule at 30 °C (spectra a and b). A number of changes are apparent beyond the line broadening anticipated due to the increase in viscosity. First, the ordering in the C, D, E region has changed from (C, D), E to D, (C, E). Second, the distribution of intensities in the J, K, L region has altered. Third, resonances N and O are virtually superimposed at 10 °C. Fourth, P has roughly doubled in intensity relative to M, and fifth, R has resolved into two features.

The NOEs obtained reveal the sequence I, N, A, (P, Q) as at 30 °C. The second helix, H, E, M, B, F, C, J, is there, but for reasons which are presently obscure while the F to C and J to C NOEs are observed, C to F and C to J are barely detectable. The D, O, Q relationship is preserved, however.

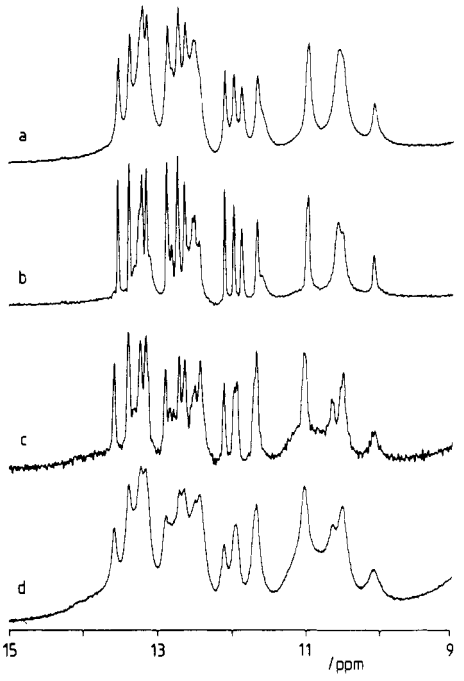

FIGURE 8: rrnB fragment at 10 and 30 °C. Five-second cycle time data were collected on the 2.5 mM rrnB fragment sample at 30 (spectrum a) and 10 °C (spectrum d) at pH 7.2. A resolution-enhanced version of the 30 °C spectrum is shown in spectrum b. Spectrum c is the resolution enhanced form of the 10 °C spectrum (spectrum d).

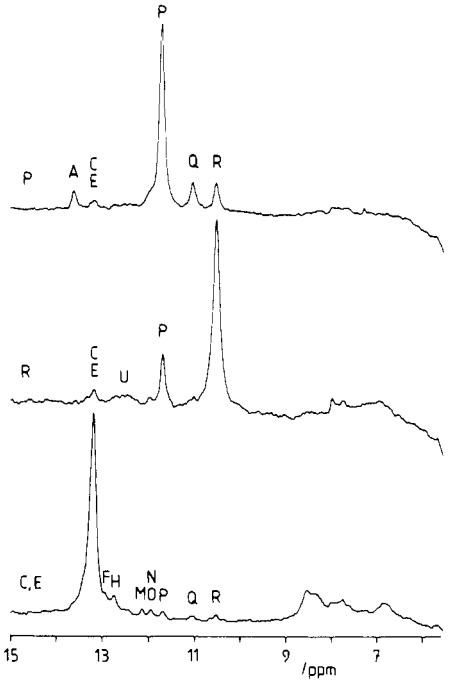

FIGURE 9: Selected NOEs of rrnB fragment at 10 °C. Except for the temperature of data acquisition, in this case 10 °C, the conditions are those described in Figure 3.

Most striking in the low temperature spectrum is the observation that presaturation of P leads to a strong NOE to the upfield component of R as well as an NOE to (C, E) (compare Figures 9 and 4). Both features are very weak at 30 °C. The upfield component of R is related by NOE to P and also to the resonance coincident with (C, E). The (C, E) NOE to P and R upfield is also evident. Similar NOEs have been observed in experiments on ribosomal fragment at 10 °C (data not shown).

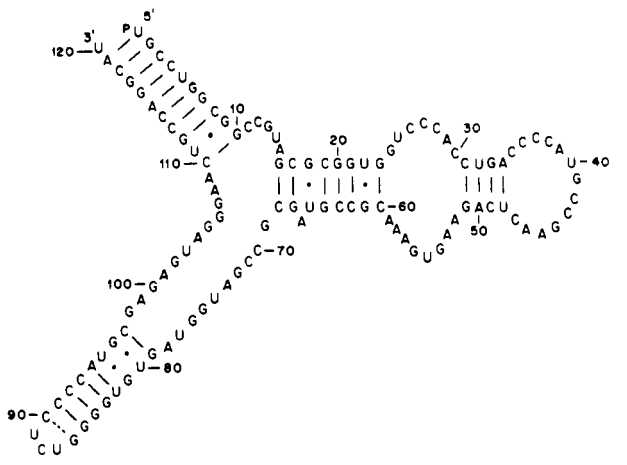

FIGURE 10: 5S RNA secondary structure. *E. coli* 5S RNA is depicted in the three-stem secondary structure form proposed by Fox & Woese (1975). The version of that structure shown here is the one recently proposed by Garrett et al. (1981). This figure is redrawn with minor modifications from Figure 1 in Garrett et al. (1981).

Given the obvious strength of the P to R relationship and the chemical shift positions, there is little doubt that R and P include imino proton resonances from a GU base pair and that a new short segment, (GU)(GC), has been found. The relationship of the (C, E) resonance picked up by the R–P GU base pair and resonances C or E in the $(GC)_3(AU)(GC)_3$ helix is uncertain. It is possible that the resonance at the (C, E) position related to R and P is resonance T seen as a broad feature at about that chemical shift in the spectrum at 30 °C.

Discussion

A large number of proposals have been made for the secondary and tertiary structure of 5S RNA. Upon completion of the sequence of *E. coli* 5S RNA, Brownlee et al. (1968) noted that the terminal bases of the molecule could be brought together to form a long helical region, the longest perfect helix possible in the molecule. All models proposed for 5S RNA include this terminal helix. It is gratifying, therefore, to find a series of resonances in the fragment spectrum which are readily interpreted as the imino proton resonances of a helical structure of sequence $(GC)_3(AU)(GC)_3$. This segment corresponds to bases 2–8 paired with bases 112–118, the middle of the terminal stem helix. There is no other place in the 5S RNA that such a series of connected resonances can be accommodated without having to invoke outrageously irregular structures (see Figure 10). No model for 5S RNA suggests an alternative structure within the fragment region which would give rise to a series of resonances of the kind observed. Thus the data presented provide strong physical evidence for the existence of the terminal stem.

The most logical position for the shorter stem, $(GC)_2$-(AU)(GU), is in the structure formed by pairing bases 81–84 with bases 92–95, the stem of the so-called "procaryotic loop" (Fox & Woese, 1975) (Figure 10). By no means all models suggested for 5S RNA include this structure or some other which would give similar NOEs. Among the models which do not contain this feature is the rod model of Brownlee et al. (1968) and the models of Cantor (1967), Boedtker & Kelling (1967), Raacke (1968), Jordan (1971), Kearns & Wong (1974), Monier (1974), and Weidner et al. (1977). In our estimation the absence of such a feature in these models invalidates them as descriptions of 5S RNA.

There is a large group of models which contain the $(GC)_2(AU)(GU)$ structure, most of them of the three stem

type advocated by Fox & Woese (1975) on comparative sequence arguments (Brownlee et al., 1968; Madison, 1968; DuBuy & Weissman, 1971; Fox & Woese, 1975; Osterberg et al., 1976; Fox & Wong, 1979; Studnicka et al., 1981; Hori & Osawa, 1979; Pieler & Erdmann, 1982). Given the strong support that the three stem secondary structure pattern finds in the available chemical data [see Douthwaite & Garrett (1981) and references therein] and these new physical data, which relate to the structure of two of the three stems, there is little doubt it is fundamentally correct whatever the tertiary structure of the molecule. It should be pointed out, however, that the four stem model of Luoma & Marshall (1978), a modest variant of the three stem models, is still viable from the standpoint of the NMR data.

Not all aspects of the Fox–Woese model, on the other hand, are confirmed. As usually drawn, the terminal stem includes an AU involving bases 1 and 119. There is no evidence for the existence of a third AU in these spectra, nor is it found by NMR in the intact molecule (unpublished data). Either that AU does not exist or its hydrogen-bonded imino proton exchanges with solvent protons too fast to give a detectable resonance. Again, as in the case of the terminal stem, the procaryotic loop stem detected in these studies is not the whole stem usually depicted. In most models the stem is extended on the $(GC)_2$ side by one or two more (GC) base pairs, for which we have no evidence by NOE.

Both stems are drawn in most secondary structure models (Figure 10) as ending on their proximal ends with (GU)(GC) base pairs. Two such sequences have been identified in the fragment spectrum, one of which is unstable at high temperatures. The absence of further NOEs frustrates the connection of these sequences to the ends of the two stems. (GU) base pairs commonly give strong NOEs to their neighbors (Hare & Reid, 1982b), and the locations for these GUs in the standard model structure are the most obvious ones available. The absence of corresponding NOEs is a puzzle. Experiments were done at reduced temperature with presaturation times up to 1 s instead of the standard 0.2 s in hopes of seeing NOEs from the helical stems to the (GU)(GC) sequences. These experiments revealed nothing in addition to what was already known from the shorter presaturation experiments. All one can offer is the hypothesis that the structures of these stems may be irregular at their putative (GU)(GC) ends, disrupting the expected NOEs by either virtue of exchange or time average geometry. The fact that the R–P (GU) is strongly temperature sensitive gives some support for such a view.

It is clear that the downfield spectrum of the fragment is not yet fully assigned. Besides the two "orphan" (GU)(GC) sequences, the data do not identify which base pairs correspond to resonances G, K, L, S, T, and U. Moreover, by its intensity resonance R represents two or three protons, but only one has been identified as to base pair type, namely, the temperature-sensitive GU imino proton. Surely some of these unassigned resonances must represent interactions responsible for structuring of the region between the terminal stem and the procaryotic loop stem so as to render it insensitive to RNase digestion. Others may in fact be adjacent to the longer helical structures already identified and fail to give NOEs, due either to exchange effects or to irregularities in their time-average geometries.

A further issue unresolved is the order of resonances in the terminal helix with respect to the sequence. The sequence found by NOE, $(GC)_3(AU)(GC)_3$, is mirror symmetric. It is our belief that J is the terminal end of the helix and H the inside end. The argument is based on the finding of a continuation of NOEs at 30 °C from H into S and thence onto T, U, and R. We do not consider this observation as proving the orientation of these resonances, however, and feel that more experimentation will be required to resolve this question, as well as the other issues mentioned. In addition it is important that further experiments be carried out to confirm (or deny) the validity of the assignments we have put forward above. Further work along these lines is certainly justified since an extension of the assignments of the fragment spectrum should reveal new facts about the structure of this molecule and, by inference, about the structure of its parent, 5S RNA.

Acknowledgments

We gratefully acknowledge the gift of *E. coli* strain HB101/pKK5-1 from Drs. J. Brosius and H. Noller. We thank B. Rennie and G. Sun for their able technical assistance. NMR spectroscopy was done at the Northeast Regional NMR facility (CHE-7916210).

References

Boedtker, H., & Kelling, D. G. (1967) *Biochem. Biophys. Res. Commun. 29*, 758–766.

Brosius, J., Dull, T. J., Sleeter, D. D., & Noller, H. F. (1981) *J. Mol. Biol. 148*, 107–127.

Brownlee, G. G., Sanger, F., & Barrell, B. G. (1968) *J. Mol. Biol. 34*, 379–412.

Burns, P. D., Luoma, G. A., & Marshall, A. G. (1980) *Biochem. Biophys. Res. Commun. 96*, 805–811.

Cantor, C. R. (1967) *Nature (London) 216*, 513–514.

Douthwaite, S., & Garrett, R. A. (1981) *Biochemistry 20*, 7301–7307.

Douthwaite, S., Garrett, R. A., Wagner, R., & Feunteun, J. (1979) *Nucleic Acids Res. 6*, 2453–2470.

DuBuy, B., & Weissman, S. M. (1971) *J. Biol. Chem. 246*, 747–761.

Fox, G. E., & Woese, C. R. (1975) *Nature (London) 256*, 505–506.

Fox, J. W., & Wong, K.-P. (1979) *J. Biol. Chem. 254*, 10139–10144.

Garrett, R. A., Douthwaite, S., & Noller, H. F. (1981) *Trends Biochem. Sci. (Pers. Ed.) 6*, 137–139.

Hare, D. R., & Reid, B. R. (1982a) *Biochemistry 21*, 1835–1842.

Hare, D. R., & Reid, B. R. (1982b) *Biochemistry 21*, 5129–5135.

Hori, H., & Osawa, S. (1979) *Proc. Natl. Acad. Sci. U.S.A. 76*, 381–385.

Jarry, B., & Rosset, R. (1971) *Mol. Gen. Genetics 113*, 43–50.

Johnston, P. D., & Redfield, A. G. (1978) *Nucleic Acids Res. 4*, 3599–3615.

Johnston, P. D., & Redfield, A. G. (1981) Biochemistry *20*, 1147–1156.

Jordan, B. R. (1971) *J. Theor. Biol. 34*, 363–378.

Kearns, D. R. (1976) *Prog. Nucleic Acid Res. Mol. Biol. 18*, 91–149.

Kearns, D. R. (1977) *Annu. Rev. Biophys. Bioeng. 6*, 477–523.

Kearns, D. R., & Shulman, R. G. (1974) *Acc. Chem. Res. 7*, 33–39.

Kearns, D. R., & Wong, Y. P. (1974) *J. Mol. Biol. 87*, 755–774.

Kearns, D. R., Patel, D., & Shulman, R. G. (1971a) *Nature (London) 229*, 338–339.

Kearns, D. R., Patel, D., Shulman, R. G., & Yamane, T. (1971b) *J. Mol. Biol. 61*, 265–270.

Kime, M. J., & Moore, P. B. (1982) *Nucleic Acids Res. 10*, 4973–4983.

Kime, M. J., & Moore, P. B. (1983) *FEBS Lett. 155*, 199-203.
Kime, M. J., Ratcliffe, R. G., Moore, P. B., & Williams, R. J. P. (1981) *Eur. J. Biochem. 116*, 269-276.
Lightfoot, D. R., Wong, K. L., Kearns, D. R., Reid, B. R., & Shulman, R. G. (1973) *J. Mol. Biol. 78*, 71-89.
Luoma, G. A., & Marshall, A. G. (1978) *Proc. Natl. Acad. Sci. U.S.A. 75*, 4901-4905.
Luoma, G. A., Burns, P. D., Bruce, R. E., & Marshall, A. G. (1980) *Biochemistry 19*, 5456-5462.
Madison, J. T. (1968) *Annu. Rev. Biochem. 37*, 131-148.
Monier, R. (1974) in *Ribosomes* (Nomura, M., Tissieres, A., & Lengyel, P., Eds.) pp 141-168, Cold Spring Harbor Laboratory, Cold Spring Harbor, NY.
Osterberg, R., Sjoberg, B., & Garrett, R. A. (1976) *Eur. J. Biochem. 68*, 481-487.
Pieler, T., & Erdmann, V. A. (1982) *Proc. Natl. Acad. Sci. U.S.A. 79*, 4599-4603.
Raacke, I. D. (1968) *Biochem. Biophys. Res. Commun. 31*, 528-533.
Reid, B. R. (1981) *Annu. Rev. Biochem. 50*, 969-996.
Reid, B. R., & Hurd, R. E. (1977) *Acc. Chem. Res. 10*, 396-402.
Reid, B. R., McCollum, L., Abeiro, N. S., Abbate, J., & Hurd, R. E. (1979) *Biochemistry 18*, 3996-4005.
Rosset, R., & Monier, R. (1963) *Biochim. Biophys. Acta 68*, 653-656.
Roy, S., & Redfield, A. G. (1981) *Nucleic Acids Res. 9*, 7073-7083.
Salemink, P. J. M., Raue, H. A., Heerschap, A., Planta, R. J., & Hilbers, C. W. (1981) *Biochemistry 20*, 265-272.
Sanchez, V., Redfield, A. G., Johnston, P. D., & Tropp, J. (1980) *Proc. Natl. Acad. Sci. U.S.A. 77*, 5659-5662.
Schimmel, P. R., & Redfield, A. G. (1980) *Annu. Rev. Biophys. Bioeng. 9*, 191-221.
Studnicka, G. M., Eisenberg, F. A., & Lake, J. A. (1981) *Nucleic Acids Res. 9*, 1885-1904.
Weidner, H., Yuan, R., & Crothers, D. M. (1977) *Nature (London) 266*, 193-194.
Wong, Y. P., Kearns, D. R., Reid, B. R., & Shulman, R. G. (1972) *J. Mol. Biol. 72*, 741-749.
Zimmermann, R. A. (1980) in *Ribosomes Structure, Function & Genetics* (Chambliss, G., Craven, G. R., Davies, J., Davis, K., Kahan, L., & Nomura, M., Eds.) pp 135-170, University Park Press, Baltimore, MD.

Nuclear Overhauser Experiments at 500 MHz on the Downfield Proton Spectra of 5S Ribonucleic Acid and Its Complex with Ribosomal Protein L25†

M. J. Kime and P. B. Moore*

ABSTRACT: The downfield (9-15 ppm) proton spectrum of *Escherichia coli* 5S RNA has been examined at 500 MHz by using nuclear Overhauser methods. The data confirm the existence of the terminal and procaryotic loop helices within the molecule [Fox, G. E., & Woese, C. R. (1975) *Nature (London) 256*, 505-506]. Very little stable, double-helical structure is detectable in the third loop of the molecule, the one comprising bases 12-68. The downfield spectrum of 5S RNA is perturbed in a highly specific manner upon addition of protein L25 to the system. The changes seen strongly suggest that the binding site for L25 on 5S RNA includes the procaryotic loop helix, but not the terminal stem helix. Similar complexes formed between L25 and the 5S RNA fragment consisting of bases 1-11, 69-87, and 89-120 show exactly the same spectral alterations. A number of downfield resonances appear in the spectra of these complexes which have no counterparts in the free RNA, suggesting the stabilization of new RNA structures by the protein. There are some indications of protein-nucleic acid nuclear Overhauser effects.

Proton nuclear magnetic resonance (NMR) techniques have been used to study the structure and properties of RNAs for over a decade [for review see Kearns & Shulman (1974); Kearns, 1976, 1977; Reid & Hurd, 1977; Schimmel & Redfield, 1980; Reid, 1981]. The tRNAs have been the subject of much of this work, but 5S RNA, the next larger abundant RNA species, has also received attention (Wong et al., 1972; Kearns & Wong, 1974; Burns et al., 1980; Luoma et al., 1980; Salemink et al., 1981). The portion of a nucleic acid proton spectrum of particular interest is the downfield region (9-15 ppm) where hydrogen-bonded base pair imino protons resonate. Powerful methods have been developed lately for assigning the downfield resonances of small nucleic acids based on the nuclear Overhauser effect (NOE) (Johnston & Redfield, 1978, 1981; Sanchez et al., 1980; Roy & Redfield, 1981; Hare & Reid, 1982a,b; Roy et al., 1982). It is clear that the problem of the assignment of the spectra of tRNAs will soon be solved in several cases.

Recently we have begun applying the NMR methods which work so well for tRNAs to the interpretation of the downfield proton spectrum of 5S RNA and its complexes with ribosomal proteins. It has been shown that the large 5S RNA fragment derived from the whole molecule by limited ribonuclease A (RNase A) digestion (Douthwaite et al., 1979) has a secondary, and probably a tertiary, structure similar to that of

† From the Department of Chemistry, Yale University, New Haven, Connecticut 06511. *Received January 3, 1983; revised manuscript received March 4, 1983.* This research was supported by a grant (to P.B.M.) from the National Institutes of Health (AI-09167). M.J.K. is a NATO/SERC postdoctoral fellow. NMR spectroscopy was done at the Northeast Regional NMR Facility which is supported by the National Science Foundation (CHE-7916210).

0006-2960/83/0422-2622$01.50/0